J Therm Anal Calorim (2009) 97:297–302
DOI 10.1007/s10973-009-0243-9

Study on thermal stability of tertiary pyridine resin

Y. Sato · A. Funakoshi · K. Okada · M. Akiyoshi ·
T. Matsunaga · S. Koyama · M. Ozawa · T. Suzuki

ICTAC2008 Conference

Abstract The fundamental properties of tertiary pyridine resin (TPR) and its mixtures with methanol/HCl and HNO_3 were investigated in order to evaluate the thermal stability of TPR and to determine the conditions necessary to avoid runaway reactions. Based on experimental DSC results, it was found that TPR with HCl was thermally stable, but strong decomposition was possible with TPR in the presence of HNO_3. From the results of heating tests on the gram scale, TPR with HNO_3 reacted violently under high temperature regardless of HNO_3 concentration and presence or absence of methanol. However, it was considered that the violent exothermic reaction could be controlled by heating temperature.

Keywords Adv.-ORIENT cycle · Tertiary pyridine resin · Methanol · Hydrochloric acid · Nitric acid · Thermal stability

Introduction

Research and development on the Fast Breeding Reactor (FBR) cycle are currently performed in Japan. The “Adv.-ORIENT” (Advanced Optimization by Recycling Instructive Elements) cycle aims to reduce environmental load and utilize useful elements as part of the R & D effort of the FBR cycle at JAEA [1]. The research target of the Adv.-ORIENT cycle is to ensure that technology for separating, transmuting and utilizing minor actinides, long-lived fission products, heating fission products and rare metals that are treated as radioactive wastes are substantiated and scientifically approved.

Recovery of uranium and plutonium, and separation of minor actinides from rare-earth elements, is performed using tertiary pyridine resin (TPR) with methanol (MeOH)/hydrochloric acid (HCl) or nitric acid (HNO_3) [1] in the Adv.-ORIENT cycle. Separation of americium, curium and plutonium (including uranium and neptunium) from spent fuel has already proven successful [2]. A chemical flowchart on multi-functional reprocessing processes has been proposed based on the above research results and safety engineering research has been initiated on the corrosive stability of structures, thermal safety and radiochemical safety of TPR [1]. There have been some explosive accidents caused by the contact of weakly basic anion exchange resins with HNO_3 [3, 4]. TPR functions as a soft donor and weakly basic anion exchange resin [5] and should therefore be treated carefully, especially in the presence of HNO_3. There is a possibility that similar

Y. Sato (✉) · A. Funakoshi · K. Okada · M. Akiyoshi ·
T. Matsunaga
Research Core for Explosion Safety, National Institute of
Advanced Industrial Science and Technology, AIST Tsukuba
Central 5, 1-1-1 Higashi, Tsukuba-shi, Ibaraki 305-8565, Japan
e-mail: yoshihiko-satou@aist.go.jp

S. Koyama
O-arai Research and Development Center, Japan Atomic Energy
Agency, 4002 Narita-cho, O-arai-machi, Ibaraki 311-1393,
Japan

M. Ozawa
Tokai Research and Development Center, Japan Atomic Energy
Agency, 2-4 Shirane Shirakata, Tokai-mura, Naka-gun,
Ibaraki 319-1195, Japan

T. Suzuki
Research Laboratory for Nuclear Reactors, Tokyo Institute
of Technology, 2-12-1 O-okayama, Meguro-ku,
Tokyo 152-8550, Japan

explosions may occur during the multi-functional reprocessing process because TPR is treated with MeOH/HCl or HNO_3 according to the proposed chemical flowchart. To maintain confinement of radioactive materials, it is critical to understand quantitatively the conditions under which fire and explosions can be avoided. While research on the thermal decomposition and stability of TPR itself has been performed [6, 7], the thermal stability of TPR with absorbed anions and mixtures of TPR with HCl or HNO_3 has not been investigated quantitatively. In this paper, fundamental properties to evaluate the thermal stability of TPR itself and mixtures of TPR with MeOH/HCl or HNO_3 were measured. Moreover, conditions necessary to avoid fire and explosions were investigated.

Experimental

Materials

TPR was synthesized at the Tokyo Institute of Technology. Figure 1 shows the structural formula of TPR [5]. The particle size was 100–200 mesh. The resin had a cross-linkage of 20%. Raw Cl-type resin (TPR-Cl) and NO_3-type resin (TPR-NO_3), with the Cl^- anion replaced by NO_3^- anion, were used in these experiments. All resins were dried in vacuum desiccators for more than 48 h. HCl (Wako Pure Chemical Industries) and HNO_3 (Tama Chemicals) were used without purification and were prepared to the prescribed concentrations by deionized water. MeOH (Wako Pure Chemical Industries) was used without purification.

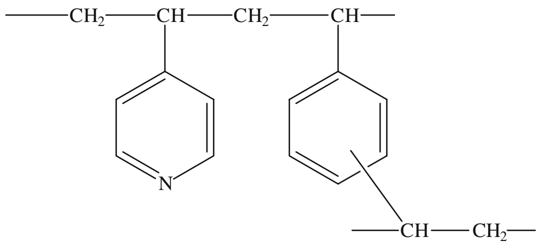

Fig. 1 Structural formula of TPR

Methods

Analysis of fundamental properties of TPR

The moisture ratio and elemental compositions (C/H/N/O) of TPR were analyzed. The moisture ratio was analyzed by HB43 (Mettler-Toledo). The quantity of sample was about 3 g. The heating device was heated to 105 °C in 1 min from the start of the analysis and the temperature was maintained to the end of the analysis. C, H and N compositions were analyzed by EA 1110 (CE Instruments). The composition of O was analyzed by Flash EA 1112 (CE Instruments). The quantity of samples was about 2 mg. Moreover, the bulk specific gravity, swelling ratio and heat of combustion were analyzed. The bulk specific gravity was analyzed by filling TPR in a commercial specific gravity bottle and weighing the bottle in an analytical balance. The swelling ratio was analyzed by feeding TPR into a 50-mL graduated cylinder, adding deionized water of about double the volume of TPR to the cylinder and letting the mixture stand for over 48 h. The heat of combustion was analyzed by IKA C2000 basic. A standard bomb C5010 was used. The oxygen pressure was 3 MPa. Samples were placed in a combustion crucible C14 directly or within two gelatin capsules.

Evaluation of thermal stability by thermal analysis

Thermal analysis by DSC was performed to investigate the thermal stability of TPR itself and mixtures of TPR/MeOH/HCl or HNO_3. A high pressure DSC 2920 (TA Instruments) was used. About 1 mg of sample was placed in a test cell. Samples were heated from room temperature to 500 °C under 0.1 MPa nitrogen atmosphere. The heating rate was 10 K min^{-1}. NETZSCH hastelloy pressure cells were used.

Evaluation of thermal stability by heating test on gram scale

In order to investigate the behavior of mixtures of TPR/MeOH/HNO_3 under heating conditions, the mixture was heated by an adiabatic furnace. The temperature was measured by thermocouples, and the appearance was observed by video camera. An adiabatic furnace was made in-house for these tests. Figure 2 shows a cross-sectional view of the adiabatic furnace. The thermal insulator was filled by an enameled vessel ($^{\phi}$250 mm * ^{h}250 mm). A stainless steel vessel ($^{\phi}$80 mm * ^{h}180 mm, ^{t}5 mm, 904 mL) was placed in the enameled vessel. A thermal insulator of about 30 mm was placed on the bottom of the stainless steel vessel in order to prevent direct heat transfer from the stainless steel. A flexible heater ($^{\phi}$1.6 mm * ^{L}1700 mm, 100 V, 500 W) was inserted spirally around the surface of the stainless steel vessel. Two thermocouples were placed on the surface of the stainless steel vessel, one of which was connected to a PID temperature controller (CHINO KP1000), and the temperature and heating rate were controlled. The temperatures at four points (sample, atmosphere of heater, surfaces of heaters No. 1 and No. 2) were measured by sheathed thermocouples (K-type, $^{\phi}$1.6 mm) and were recorded on a data

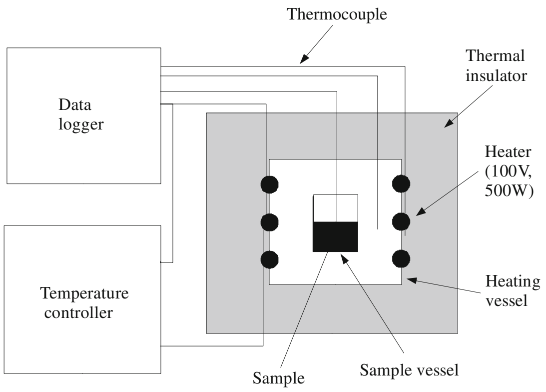

Fig. 2 Cross-sectional view of adiabatic furnace

Table 1 Experimental condition of heating tests on gram scale

No.	TPR/g	MeOH/g	HNO_3/g	HNO_3/M	Heater/°C
1	10	24	6	15	220
2	10	24	6	8	220
3	10	24	6	3	220
4	10	24	6	15	170
5	10	0	6	15	220

logger (OMRON ZR-RX40). The thermocouple for measuring sample temperature was covered by PTFE in order to prevent corrosion by acid. Samples were placed in glass test tubes ($^{\phi}$30 mm * ^{h}200 mm). The upper part of the test tube was recorded by video camera for a prescribed time. Table 1 shows experimental conditions for the heating tests.

Analysis of reaction products by spectroscopy

FT-IR spectroscopy was performed in order to investigate chemical denaturing of the samples after heating tests on a gram scale. A SpGX/Raman FT-IR system (Perkin-Elmer) was used. ATR-FT-IR was performed by Durascope (SensIR Technologies). Samples were crushed by agate mortar and placed on the diamond window of the ATR unit. Uniform distribution of the samples was verified by enlarging the image. The wavenumber range measured was 4,000 cm^{-1} to 400 cm^{-1} with a resolution of 4 cm^{-1}. Spectra were obtained by integrating 64 times.

Results and discussion

Analysis of fundamental properties of TPR

The moisture ratio of TPR-Cl was 7.74% and that of TPR-NO_3 was 6.02%. TPR absorbed water strongly regardless of drying conditions. Table 2 shows the elemental compositions of TPR. The molar mass was obtained based on these measurements and the oxygen balance [8] was calculated. The oxygen balance of TPR-Cl was determined to be −237 and that of TPR-NO_3 was −168. Since these results were far below zero, it was expected that TPR itself possessed little risk for explosion. The bulk specific density of TPR was 0.34. TPR swelled about triply in water vs. dry conditions. The heat of combustion of TPR was 26.62 ± 0.71 kJ/g ($n = 3$).

Table 2 Elemental compositions of TPR

Type	C/%	H/%	N/%	O/%	Molar mass	Oxygen balance
TPR-Cl	4.99	6.54	0.59	0.64	85.03	−237
TPR-NO_3	4.58	5.52	0.91	1.56	98.21	−168

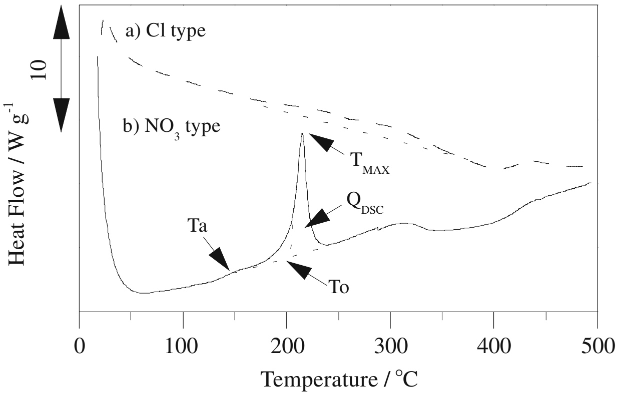

Fig. 3 DSC curves of TPR-Cl and TPR-NO_3

Table 3 Measurement results of TPR-Cl and TPR-NO_3 by DSC

Type	T_a/°C	T_o/°C	T_{MAX}/°C	Q_{DSC}/J g^{-1}
TPR-Cl	187	197	302	376
TPR-NO_3	152	202	215	816

Evaluation of thermal stability by thermal analysis

Figure 3 shows DSC curves of TPR-Cl and TPR-NO_3. Table 3 shows temperatures where the DSC curve deviates from the baseline (T_a), exothermic onset temperature (T_o), maximum peak temperature (T_{MAX}) and heat of reaction (Q_{DSC}) of TPR-Cl and TPR-NO_3. TPR-Cl decomposed slightly while T_a of TPR-NO_3 was lower and Q_{DSC} of TPR-NO_3 was larger than that of TPR-Cl. This shows that TPR-NO_3 decomposed more violently than TPR-Cl.

Figure 4 shows DSC curves of mixtures of TPR-Cl/MeOH/1 M HCl. Significant endothermic and exothermic

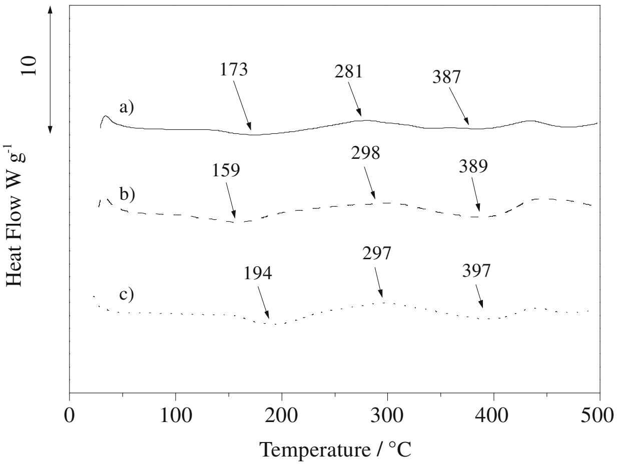

Fig. 4 DSC curves of mixture of TPR-Cl/Methanol/1 M HCl (mass ratio); (a) TPR:MeOH:HCl = 25:37:37, (b) TPR:MeOH:HCl = 25:53:22 (c) TPR:MeOH:HCl = 25:22:53

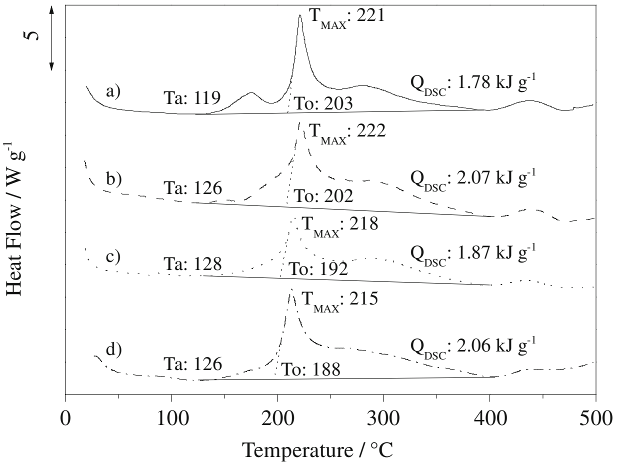

Fig. 5 DSC curves of mixture of TPR-NO$_3$/MeOH/8 M HNO$_3$ (mass ratio); (a) TPR:MeOH:HNO$_3$ = 25:22:53, (b) TPR:MeOH:HNO$_3$ = 25:37:37, (c) TPR:MeOH:HNO$_3$ = 25:53:22, (d) TPR:MeOH:HNO$_3$ = 25:60:15

reactions were not observed despite changing the mass ratio of each substance. Moreover, the DSC curves did not change.

Figure 5 shows DSC curves of mixtures of TPR-NO$_3$/MeOH/8 M HNO$_3$. A large exothermic reaction was observed unlike the case of TPR-Cl. This indicated that a strong exothermic reaction of TPR was possible in the HNO$_3$ system. T$_a$, T$_{MAX}$ and Q$_{DSC}$ did not change systematically despite changing the mass ratio of each substance. T$_o$ tended to decrease with an decrease of HNO$_3$ in the mixture.

Therefore, TPR was found to be stable thermally in the HCl system, but strong decomposition was possible in the HNO$_3$ system.

Evaluation of thermal stability by heating test on a gram scale

Table 4 shows the onset temperature, highest temperature, observed phenomena in experiments and condition of residue after tests. Test time refers to the time between the start and end times of the data logger. Onset temperature is the defined sample temperature where a sudden increase is observed by eye.

Sudden exothermic heat and release of fumes were observed with a mixture of TPR-NO$_3$/MeOH/HNO$_3$ when the temperature of the heater reached 220 °C regardless of the HNO$_3$ concentration. For example, Fig. 6 shows the temperature profile and appearance of the release of fumes in test No. 1. The sample temperature remained at 70 °C, indicating evaporation of MeOH. Then the temperature increased slowly to 175 °C followed by a sudden increase in temperature. Evaporation of HNO$_3$ solution was not observed. The onset time tended to be short with an increase of HNO$_3$ concentration while the onset temperature tended to increase with HNO$_3$ concentration. The sample temperature was kept at 155 °C and violent exothermic heat and release of fumes were not observed when the heater temperature was held at 170 °C. Therefore, the temperature where the mixture starts a runaway reaction was found to be 155 °C to 175 °C on the gram scale. Moreover, it was considered that the violent exothermic reaction could be controlled by heating temperature.

In the case of a mixture of TPR-NO$_3$/HNO$_3$, the sample temperature was held at 105 °C. The sample temperature increased gradually, showing evaporation of the HNO$_3$ solution. After that, the sample temperature increased suddenly at 142 °C. Therefore, it was expected that MeOH was not correlated with the violent exothermic reaction.

Analysis of reaction products by spectroscopy

Figure 7 shows FT-IR spectra of TPR-Cl, TPR-NO$_3$, residue of heating mixture of TPR-NO$_3$/HNO$_3$ and residue of heating mixture of TPR-NO$_3$/MeOH/HNO$_3$. In the case of TPR-Cl, absorption bands at 1,609 cm^{-1} and 1,505 cm^{-1} were observed, which were assigned to vibrations of the phenyl ring [9]. Moreover, an absorption band at 1,636 cm^{-1} was assigned to the vibration of the pyridinium ion ring [9]. In the case of TPR-NO$_3$, a strong broad absorption band at 1,316 cm^{-1} was observed along with absorption bands from the phenyl and pyridinium ion rings. This strong absorption band was assigned to the vibration of monodentate NO$_3^-$ anion [10]. On the other hand, for the mixtures of TPR-NO$_3$/HNO$_3$ and TPR-NO$_3$/MeOH/HNO$_3$, absorption bands at 1,596 cm^{-1} and 1,507 cm^{-1} were assigned to vibrations of the phenyl ring and absorption bands at 1558 cm^{-1}, 1490 cm^{-1} and 1413 cm^{-1} were assigned to vibrations of

Table 4 Observed phenomena on heating tests on gram scale

No.	Test time/min	Onset temperature/°C	Onset time/min	Highest temperature/°C	Observed phenomena	Condition of residue
1	138	175	78	317	Release of fume	Black solid
2	85	167	81	330	Release of fume	Black solid
3	143	156	132	286	Release of fume	Black solid
4	5701	None	None	155	None	Black solid
5	190	142	182	280	Release of fume	Black solid

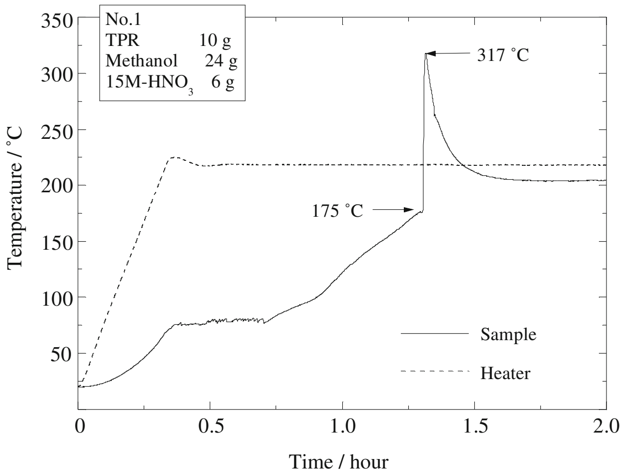

Temperature profile

Appearance of release of fume

Fig. 6 Temperature profile and appearance of release of fume in heating test on gram scale

the pyridine ring [9]. Absorption bands from the vibrations of the pyridinium ion ring and NO_3^- anion disappeared. Therefore, it is considered that NO_3^- absorbed TPR is desorbed and the pyridinium ion is deionized to a pyridine ring. Moreover, a weak absorption band at 1,684 cm^{-1} was assigned to a carbonyl group. It is known that nitration and oxidation of alkyl benzene occurs by nitric acid [11]. Therefore, it was concluded that the hard exothermic reactions observed in the heating test on a gram scale were oxidation, generation of nitro compounds by HNO_3 and subsequent decomposition.

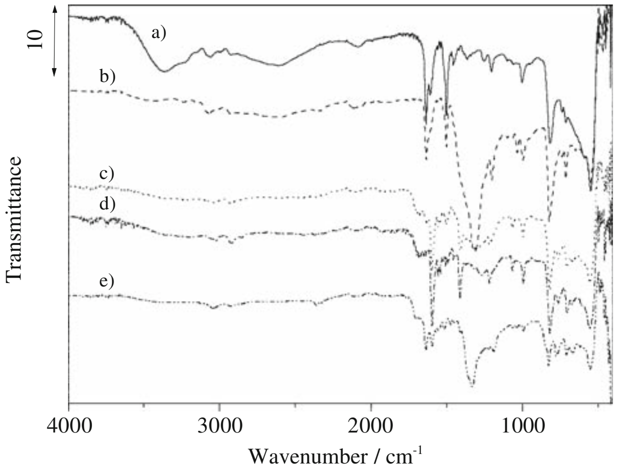

Fig. 7 FT-IR spectra of TPR and residues after heating test on gram scale (a) TPR-Cl, (b) TPR-NO_3, (c) residue of heating test No. 1, (d) residue of heating test No. 4, (e) Residue of heating test No. 5

Conclusions

Fundamental data to evaluate thermal stability of TPR and mixtures of TPR with MeOH/HCl or HNO_3 were measured. Moreover, conditions necessary to avoid fire and explosions were investigated. The molar mass was obtained based on elemental analysis results (C/H/N/O) and the oxygen balance was found to be far below zero. Therefore, it is expected that TPR itself possesses little explosive hazard. From the results of DSC analysis, it was found that TPR was stable thermally in the HCl system, but strong decomposition was possible in the HNO_3 system. From the heating tests on a gram scale, violent reaction occurred in TPR under high temperature in the HNO_3 system. The reaction occurred regardless of HNO_3 concentration and presence or absence of MeOH. However, it was confirmed that the reaction did not occur when the heating temperature decreased. Moreover, it was considered that the violent exothermic reaction could be controlled by heating temperature. From the results of FT-IR spectroscopy, it was concluded that the reaction consisted of oxidation, generation of nitro compounds by HNO_3 and subsequent decomposition.

Acknowledgements We thank the AIST technical center that provided great technical support in performing analysis of elemental compositions (C/H/N/O) of TPR. This work was supported by funded research from the Japan Atomic Energy Agency (JAEA).

References

1. Ozawa M, Suzuki T, Koyama S, Akatsuka H, Mimura H, Fujii Y. A new back-end cycle strategy for enhancing separation, transmutation and utilization of materials (Adv.-ORIENT cycle). Prog Nucl Energy. 2008;50:476–82.
2. Koyama S, Ozawa M, Suzuki T, Fujii Y. Development of a multifunctional reprocessing process based on ion-exchange method by using tertiary pyridine-type resin. J Nucl Sci Technol. 2006;43:681–9.
3. Miles FW. Ion-exchange-resin system failures in processing actinides. Nucl Saf. 1968;9:394–406.
4. Calmon C. Explosion hazards of using nitric acid in ion-exchange equipment. Chem Eng. 1980;87:271–4.
5. Suzuki T, Fujii Y, Koyama S, Ozawa M. Nuclide separation from spent nuclear fuels by using tertiary pyridine resin. Prog Nucl Energy. 2008;50:456–61.
6. Li XG. High-resolution thermogravimetry of poly(4-vinylpyridine-codivinylbenzene). React Funct Polym. 1999;42:53–8.
7. Howell BA, Odelana Adeyinka O. Stability of vinylidene chloride copolymers containing 4-vinylpyridine units: thermogravimetric assesment. J Therm Anal Calorim. 2007;89(2):449–52.
8. Meyer R, Köeler J, Homburg A. Explosives. 6th ed. Weinheim: Wiley-VCH Verlag GmbH; 2007. p. 240.
9. Qu S, Zhang XW, Gao Y, You JB, Fan YM, Yin ZG, et al. Composition deviation of arrays of FePt nanoparticles starting from poly(styrene)-poly(4-vinylpyridine) micelles. Nanotechnology. 2008;19:1–7.
10. Nakamoto K. Infrared and Raman spectra of inorganic and coordination compounds. 4th ed. New York: Wiley; 1986. p. 256.
11. Titov AI. The free radical mechanism of nitration. Tetrahedron. 1963;19:557–80.